

Learning based Quality Indicator Aiding Heart Rate Estimation in Wrist-Worn PPG

E. Lutin, D. Biswas, N. Simoes-Capela, C. Van Hoof and N. Van Helleputte

Abstract— Technological advancements and miniaturization of wearable sensors have enabled long-term pervasive physiological monitoring. Wrist-worn photoplethysmography (PPG) sensors, although quite popular owing to their form factor, suffer from poor signal quality in ambulatory settings due to motion artifacts. This affects the reliable estimation of vital cardiac parameters, especially during motion/activities of daily living. Hence, in this paper, we have developed a learning-based quality indicator engine (QIE), evaluating on 23 PPG records of the TROIKA database. The engine comprises the fundamental steps of frequency-domain feature extraction, feature selection and classification by an ensemble of decision trees, achieving an accuracy of 83% in the testing set. To the best of our knowledge, the proposed quality engine is the first to be evaluated on wrist-PPG data acquired during various physical activities and with respect to improvement in heart rate (HR) estimation. The QIE demonstrated an average improvement of 43% in HR estimation, when used in conjunction with state-of-the-art WFPV algorithm.

Clinical Relevance— The proposed quality indicator engine helps to increase the efficacy of vital parameter estimation (e.g. heart rate) from pervasive, wrist-worn PPG sensors on the backdrop of motion artifacts when used in ambulatory settings (e.g. activities of daily living).

I. INTRODUCTION

Photoplethysmography (PPG) is a low-cost, non-invasive, optical technique used to detect blood volume changes in the microvascular tissue bed, measured from the skin surface. PPG signals are obtained from pulse oximeters, which emit light (using a light emitting diode) on the skin and measure (using a photodiode) the miniature variations in reflected or transmitted light intensity. The periodicity of the reflected/transmitted light corresponds to the cardiac rhythm, often used for heart rate estimation [1], [2]. While ECG is more established and robust for monitoring vital cardiac parameters, it requires the presence of ground and reference sensors placed on the chest making it inefficient in terms of wearability for daily life usage. PPG sensors provide a convenient solution as they can be acquired from peripheral positions such as earlobes, fingertips or wrist, with the latter considered as a convenient position for unobtrusive daily use. It has traditionally been used in controlled settings (clinical and home environment) in commercially available medical devices for oxygen saturation, blood pressure monitoring and cardiac activity assessing autonomic function and peripheral vascular disease [3]. With

advancements in internet of things (IoT) and wireless sensor networks (WSN) technologies, there has been a growing thrust to incorporate PPG sensors in daily life, capable of use in ambulatory settings. However, the acquisition is vulnerable to motion artifacts (MA) in daily living conditions and correspondingly distorts the signal fidelity and inhibits the robustness of the vital parameters estimated. On this backdrop, heart rate (HR) estimation, using wrist-worn PPG acquired under the influence of physical activity, has received considerable research attention, following the IEEE Signal processing competition (SPC), 2015 [1].

A host of techniques have been proposed to remove or attenuate MA using time-frequency domain signal processing - adaptive filtering [4], Kalman filtering [5], Wiener filtering & Phase vocoder (WFPV) [6], [7], empirical mode decomposition (EMD) [8], spectral subtraction [9] and learning algorithms [10]–[12]. The WFPV [6] algorithm proved to be computationally efficient, producing an error of 1.02 BPM when evaluated on the same set of signals. Most reported research on wrist PPG, have been reviewed in [13]. However, majority of the research effort and its associated success has been primarily restricted to estimating average HR every 2 seconds from 8 seconds of windowed PPG signal. It has not been possible to measure instantaneous HR from wrist-worn PPG signals acquired in ambulant environment, except two recent research efforts, which proposed an Empirical Mode Decomposition and Hilbert Transform based framework [14] and convolution neural networks [15]. Similarly, the research on disease prognosis using wrist-PPG has also been limited, with a few recent papers focusing primarily on Atrial Fibrillation, the most common cardiac arrhythmia in clinical practice [16]. Disease prognosis requires a near-accurate estimation of heart rate variability (HRV) which is challenging given the inherent effect of MA. Hence, it is quintessential to formulate a quality indicator for verifying the fidelity of ambulant-PPG signals which can help in removing/neglecting corrupted frames (windows). This would aid in separating the noise/MA affected segments from clean data and further help in estimation of vital parameters.

PPG signal quality has been researched upon briefly, using time-domain metrics and learning based approaches. A dynamic time warping and multi-layer perceptron-based approach was adopted to classify against normal/arrhythmic events [17]. Similarly, a signal quality indicator was

* This work was supported by a PhD fellowship from the Research Foundation - Flanders (FWO) awarded to E. Lutin (1SB4719N).

E. Lutin, N. Simoes-Capela and C. Van Hoof are with the Department of Electrical Engineering (ESAT), KU Leuven, Kasteelpark Arenberg 10, Leuven, Belgium.

All authors are with imec, Kapeldreef 75, Leuven, Belgium (email: {Dwaipayana.Biswas, Chris.VanHoof, Nick.VanHelleputte}@imec.be)

developed for both PPG and ECG based on thresholding and template matching, identifying good/'bad' signal windows, verified against the estimation of respiratory rate [18]. An irregular pulse detection algorithm was proposed in [19], using a metric, amplitude interval ratio (AIR) which incorporates the influence of pulse amplitude fluctuation by respiration and autonomic nervous system, wherein this metric remains constant for the former while shows variability for the later. However, these approaches have been evaluated on finger-PPG where the signal morphology due to MA are quite different in comparison to wrist-PPG. In a recent study, a collection of databases, including wrist-PPG databases such as the SPC dataset [1], was used to perform PPG signal quality assessment [20]. The proposed method used five hierarchical decision rules with three features to classify: 1) pulse-free segments, 2) MA-corrupted segments and 3) noise-free PPG segments. During training, all wrist-PPG was directly labelled as MA-corrupted segments without further analysis. In another recent study, an SVM classifier was built to perform binary quality assessment in presence of Atrial Fibrillation on finger-PPG data. The resulting classifier was tested on wrist-PPG data with high accuracy [21]. However, as most PPG research, the data were collected from patients admitted to an intensive care unit, which is not representative of daily living conditions. Finally, in a study using wrist-PPG data collected in a 24h period from participants performing their daily routines, a Random Forest classifier was used to classify 5 classes of quality. However, the classification result was not further evaluated with respect to a clinical outcome (e.g. heart rate estimation or disease detection) [22].

One of the pre-requisites for cardiac monitoring is to ensure long-term continuous operation of the battery-powered resource constrained sensor nodes. Analyzing the data on the sensor node yields an energy efficient solution in comparison to continuous transmission of raw data to a remote server [23]. This necessitates low-complexity processing, ensuring energy efficient operation of the sensor nodes for longer duration. In this work, we have developed a low-complexity supervised learning based, quality indicator engine (*QIE*), which can identify good/bad PPG frames. The *QIE* was evaluated on the 22 SPC records and further validated in conjunction with a state-of-the-art HR estimation algorithm (WFPV), demonstrating an improvement in overall results of the testing set. The paper is structured as follows: the proposed methodology using our learning-based approach is described in section II, the results and analysis have been presented in section III and conclusions have been drawn in section IV.

II. QIE METHODOLOGY

Recent research developments have made HR estimation possible from PPG data collected during intense physical motion. Our proposed *QIE*, is envisaged as a pre-processing stage to vital parameter estimation (in this case HR), to have robust estimates as illustrated in Fig. 1. The engine is based on ECG-assisted supervised learning framework, wherein we threshold HR estimation differences between PPG and ECG as the basis for ground truth labelling. Once trained, the model is

prospectively evaluated on test PPG data to identify good/bad signal frames (i.e. windows). The identified good frames are processed to estimate HR, while the bad frames are dropped, saving much needed computation resource. Hence, our proposed *QIE* is a predecessor to vital parameter estimation.

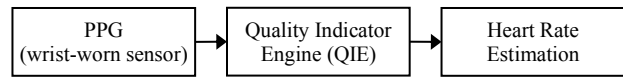


Figure 1. Envisaged use-case for *QIE*, aiding HR estimation from wrist-worn, motion artifact induced PPG signals.

The *QIE* was developed in conjunction with a state-of-the-art WFPV HR estimation algorithm and evaluated on the SPC database. The algorithm uses Wiener filtering to attenuate MA in PPG using noise signatures from acceleration data followed by phase vocoder for refining HR estimates and an adaptive post-processing step. The publicly available IEEE SPC dataset comprises 23 recordings of 20 subjects, age ranging 18 to 58, performing three different activities. All recordings were captured with a 2-channel pulse oximeter with green LEDs, a tri-axial accelerometer and a chest ECG for the ground-truth HR estimation. All channels were sampled at 125 Hz and the data were transmitted to a computer using Bluetooth. Subjects 1 to 12 performed activity T1 which involved walking/running protocol on a treadmill with the following speeds: 1–2 km/h for 0.5 min, 6–8 km/h for 1 min, 12–15 km/h for 1 min, 6–8 km/h for 1 min, 12–15 km/h for 1 min, and 1–2 km/h for 0.5 min. Subjects 14, 15, 18 and 20 performed T2 activity which consisted of various arm exercises (e.g., stretch, jump, etc.) without any specific protocol. Further, subjects 15 to 19 performed arm-intensive activities (e.g. boxing). Therefore, the entire dataset has 23 records where some subjects performed more than one activity.

In this study, the two-channel PPG signals and three-axis acceleration signals were segmented into a series of 8-second sliding time windows (with 6s overlap), following the segmentation of the ground-truth HR. The WFPV algorithm [6] was applied to all windows separately. The resulting HR of each window was compared with the ground-truth HR provided in the SPC dataset. The average absolute error (AAE) between ground-truth ECG HR and PPG HR was used to set a threshold (3 BPM) to label good/bad quality windows. An overview of the labelling process is depicted in Fig. 2. The labels were used for a supervised learning approach, which is shown in Fig. 3.

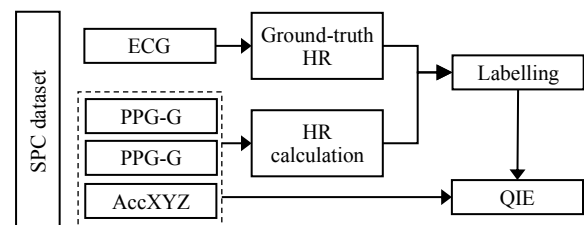


Figure 2. *QIE*: overview of the labelling process.

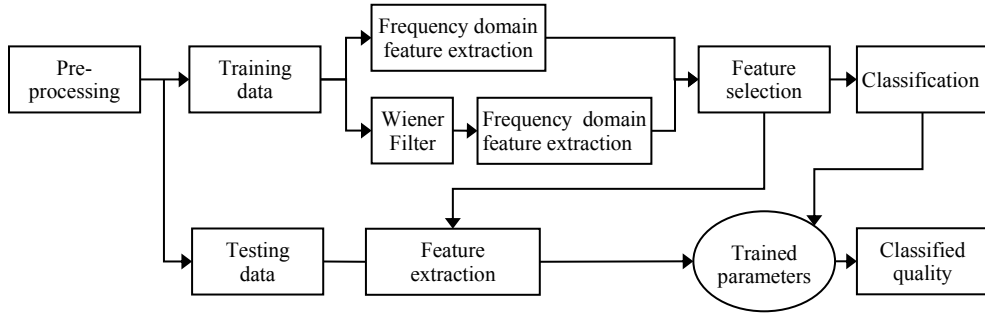


Figure 3. *QIE*: overview of the proposed supervised learning approach.

1) Pre-processing

After segmentation, all signals were filtered with a 4th order Butterworth bandpass filter with cut-off frequencies of 0.4 Hz and 4Hz, in order to cover the HR range between 0.6 and 3.3 Hz when resting and engaging in physical activities. After z-score normalization, the two-channel PPG signals were averaged into a single channel signal. The averaged signal and three-axis accelerometer signals were then down-sampled from 125 Hz to 25 Hz.

2) Feature extraction

In total, six frequency domain features were extracted from the pre-processed data to quantify characteristics inherent to PPG quality. The features included both time-invariant and time-variant features. Besides frequency band related features, e.g. the power below 1 Hz, we included the crest factor of the spectrum following the work of [7]. The crest factor reflects the prominence of a spectral peak and is calculated by

$$CF = \frac{x_{\text{peak}}}{x_{\text{rms}}} \quad (1)$$

where x_{peak} and x_{rms} are the peak value and the root-mean-squared value from the spectrum, respectively.

Additional time-invariant frequency features were obtained after Wiener-filtering (WF) as depicted in Fig. 3. A Wiener filter estimates a clean signal $S(f)$ from an observed noisy process $X(f)$, assuming a known stationary signal and an additive noise spectrum $N(f)$ [24]. The estimation of the clean signal can be obtained as

$$\bar{S}(f) = X(f) - N(f) = \left(1 - \frac{N(f)}{X(f)}\right)X(f) = W(f)X(f). \quad (2)$$

The filter convolution in the time domain equals a multiplication in the frequency domain. Hence, the Wiener filter attenuates frequencies which are more affected by the noise. The frequency-domain Wiener filter is given as

$$W(f) = \frac{P_{XX}(f) - P_{NN}(f)}{P_{XX}(f)} = \frac{P_{SS}(f)}{P_{SS}(f) - P_{NN}(f)}. \quad (3)$$

Following [6], we estimated the noise spectrum $P_{NN}(f)$ from the three accelerometer signals by averaging their spectra and the clean PPG spectrum $P_{SS}(f)$ from the previous filter outputs in a recursive manner. The final filter coefficients were included as features, as well as the crest-factor after filtering. Table I presents a description of all the features.

TABLE I. DESCRIPTION OF EXTRACTED FEATURES

Domain	Features	Explanation
Time-invariant frequency features (before WF)	powerNoise	Spectral power below 1Hz
	CF	Crest factor; ratio of the spectral peak and the root mean square of the spectrum
Time-variant frequency features	coeNoise	Sum of scalogram coefficients below 1Hz
	CF-t	Mean time-variant crest factor
Time-invariant frequency features (after WF)	meanWF	mean of Wiener filter coefficient
	CF-filtered	Crest factor after Wiener-filtering

3) Feature selection

The best features were selected using the feature selection technique of Minimum Redundancy Maximum Relevance (MRMR). The mutual information of variables is used to quantify the redundancy and relevance to the response variable [25]. The top two features were CF-filtered and powerNoise.

4) Classification

The selected features were used in an ensemble learner: Random Under-Sampling Boosted (RUSBoosted) Trees. RUSBoost is designed to improve the classification performance of a weak learner, such as a decision tree, and is effective at classifying imbalanced data [26]. The number of trees and number of decision nodes within each tree were optimized with respect to five-fold cross-validation via a grid search in the training data. The resulting classifier included 500 trees with each having 33 nodes. The learning rate was set to 0.1. The dataset consisted of 3203 8s-windows and was randomly split (80%-20%) into training and testing data, resulting in a training set of 2562 windows and a test set of 641 windows. The classification results, selected features and a corresponding detailed analysis are presented in the following section.

III. RESULTS AND ANALYSIS

The performance of the classifier on the testing data is reported in Table II.

TABLE II. CLASSIFICATION RESULTS

	Accuracy	Sensitivity	Specificity	F1 score	Precision
Classifier	0.8253	0.6854	0.8478	0.5214	0.4207

A. QIE and Heart Rate estimation

The quality indicator engine (feature extractor, selection and classification) was further applied on the testing data. All windows classified as bad quality were removed to improve the effective HR estimation result. Table III details the number of windows before and after application of the QIE, together with the average absolute error (AAE) and the standard deviation of the absolute error (SDAE). The QIE was able to discard 145 8s-windows out of 641 8s-windows, resulting in an improvement of 43% in HR estimation. In a real-time setting, the removal of these bad quality windows, prior to HR estimation, would have resulted in a more energy efficient operation of the wearable system, displaying a real-time HR.

TABLE III. EFFECT OF QIE AS A PREDECESSOR TO HR ESTIMATION

Before QIE		After QIE	
Number of windows	AAE \pm SDAE	Number of windows	AAE \pm SDAE
641	2.00 \pm 3.54	496	1.14 \pm 1.57

B. Complexity Analysis

Given the use-case of the proposed work on wrist-worn ambulant PPG, it is rather essential to ensure that the QIE can perform fast inference such that it does not cause a delay in post-processing of vital parameters. The QIE involves extracting two features using FFT (complexity $O(M\log N)$, where N is the data size, i.e. 256 in our case), the classification uses a Decision tree algorithm (complexity $O(kM\log N)$, where k is the number of features, i.e. 2 in our case). This makes the QIE implementation amenable for real-time inference.

IV. DISCUSSION

Quality metrics for ECG have been extensively explored and acknowledged for their ability to reduce false alarms in diagnostic tools [27]. Analogously, there have been several papers reported on signal quality estimation of PPG signals, though majority of which are based on finger PPG signals [17], [18], [28]–[32]. Regarding wrist PPG, the focus has been primarily on denoising the MA-affected PPG signal, rather than devising a signal quality indicator. Table IV gives an overview of recent studies using a variety of denoising algorithms on the SPC dataset.

The proposed study was aimed to develop a low-complexity quality indicator engine (QIE) for MA-affected PPG. The current study is unique as it combines QIE and the WFPV algorithm [6]. Using solely the WFPV algorithm, a AAE of 2.00 BPM was obtained within the test set, which is similar to the AAE reported by [6] over all 23 subjects (1.97 \pm 2.48). By applying the QIE prior to the WFPV algorithm, the AAE of the test set was reduced to 1.14 BPM while saving computation on bad frames/windows. Therefore, the proposed method outperforms some of the methods reported in Table IV. In future work, the QIE could be combined with any of these methods, reducing the AAE even further.

TABLE IV. PERFORMANCE COMPARISON IN AAE

Published work	SPC records	AAE	SDAE
Galli et al. (2018) [33]	22 subjects	2.45	2.83
Mashhadi et al. (2018) [34]	23 subjects	2.15	-
Biswas et al. (2019) [10]	22 subjects	1.47	3.37
Motin et al. (2019) [35]	23 subjects	1.85	1.57
Chung et al. (2020) [12]	23 subjects	0.76	-
Arunkumar et al. (2020) [36]	23 subjects	1.89	2.64
Proposed	20% of 23 subjects	1.14	1.57

V. CONCLUSION

This paper reports a first of its kind exploration to develop an engine that determines the signal quality for wrist-worn PPG signals. As proof-of-concept, we have demonstrated the efficacy of the engine, using it as a predecessor to improve the error rate for HR estimation. Identifying and dropping bad signal frames could also help to extract beat-to-beat information for HRV, a key component for cardiovascular disease detection. The dropped frames would need to be substituted by a running average of preceding beats. This would also save computation effort on discarded frames with poor signal quality. The resource requirement for each stage of QIE (feature extraction, classification), the key components of the engine have been chosen with an eye towards computation complexity, demonstrates the feasibility for real-time operations.

REFERENCES

- [1] Z. Zhang, Z. Pi, and B. Liu, "TROIKA: A general framework for heart rate monitoring using wrist-type photoplethysmographic signals during intensive physical exercise," *IEEE Trans. Biomed. Eng.*, vol. 62, no. 2, pp. 522–531, 2015.
- [2] Z. Zhang, "Photoplethysmography-based heart rate monitoring in physical activities via joint sparse spectrum reconstruction," *IEEE Trans. Biomed. Eng.*, vol. 62, no. 8, pp. 1902–1910, 2015.
- [3] J. Allen, "Photoplethysmography and its application in clinical physiological measurement," *Physiol. Meas.*, vol. 28, no. 3, p. R1, 2007.
- [4] M. B. Mashhadi, E. Asadi, M. Eskandari, S. Kiani, and F. Marvasti, "Heart rate tracking using wrist-type photoplethysmographic (PPG) signals during physical exercise with simultaneous accelerometry," *IEEE Signal Process. Lett.*, vol. 23, no. 2, pp. 227–231, 2015.
- [5] B. Lee, J. Han, H. J. Baek, J. H. Shin, K. S. Park, and W. J. Yi, "Improved elimination of motion artifacts from a photoplethysmographic signal using a Kalman smoother with simultaneous accelerometry," *Physiol. Meas.*, vol. 31, no. 12, p. 1585, 2010.
- [6] A. Temko, "Accurate heart rate monitoring during physical exercises using PPG," *IEEE Trans. Biomed. Eng.*, vol. 64, no. 9, pp. 2016–2024, 2017.
- [7] H. Chung, H. Lee, and J. Lee, "Finite state machine framework for instantaneous heart rate validation using wearable photoplethysmography during intensive exercise," *IEEE J. Biomed. Heal. Informatics*, vol. 23, no. 4, pp. 1595–1606, 2018.
- [8] E. Khan, F. Al Hossain, S. Z. Uddin, S. K. Alam, and M. K. Hasan, "A robust heart rate monitoring scheme using photoplethysmographic signals corrupted by intense motion artifacts," *IEEE Trans. Biomed. Eng.*, vol. 63, no. 3, pp. 550–562, 2015.
- [9] S. Salehizadeh, D. Dao, J. Bolkhovskoy, C. Cho, Y. Mendelson, and K. H. Chon, "A novel time-varying spectral filtering algorithm for reconstruction of motion artifact corrupted heart rate signals during

- intense physical activities using a wearable photoplethysmogram sensor,” *Sensors*, vol. 16, no. 1, p. 10, 2016.
- [10] D. Biswas *et al.*, “CorNET: Deep learning framework for PPG-based heart rate estimation and biometric identification in ambulant environment,” *IEEE Trans. Biomed. Circuits Syst.*, vol. 13, no. 2, pp. 282–291, 2019.
- [11] M. Essalat, M. B. Mashhadi, and F. Marvasti, “Supervised heart rate tracking using wrist-type photoplethysmographic (PPG) signals during physical exercise without simultaneous acceleration signals,” in *2016 IEEE Global Conference on Signal and Information Processing (GlobalSIP)*, 2016, pp. 1166–1170.
- [12] H. Chung, H. Ko, H. Lee, J. Lee, and S. Member, “Deep Learning for Heart Rate Estimation From Reflectance Photoplethysmography With Acceleration Power Spectrum and Acceleration Intensity,” *IEEE Access*, vol. 8, pp. 63390–63402, 2020, doi: 10.1109/ACCESS.2020.2981956.
- [13] D. Biswas, N. Simões-Capela, C. Van Hoof, and N. Van Helleputte, “Heart rate estimation from wrist-worn photoplethysmography: A review,” *IEEE Sens. J.*, vol. 19, no. 16, pp. 6560–6570, 2019.
- [14] D. Jarchi and A. J. Casson, “Towards photoplethysmography-based estimation of instantaneous heart rate during physical activity,” *IEEE Trans. Biomed. Eng.*, vol. 64, no. 9, pp. 2042–2053, 2017.
- [15] L. Everson *et al.*, “BioTranslator: Inferring R-Peaks from Ambulatory Wrist-Worn PPG Signal,” in *2019 41st Annual International Conference of the IEEE Engineering in Medicine and Biology Society (EMBC)*, 2019, pp. 4241–4245, doi: 10.1109/EMBC.2019.8856450.
- [16] S. P. Shashikumar, A. J. Shah, Q. Li, G. D. Clifford, and S. Nemat, “A deep learning approach to monitoring and detecting atrial fibrillation using wearable technology,” in *2017 IEEE EMBS International Conference on Biomedical & Health Informatics (BHI)*, 2017, pp. 141–144.
- [17] Q. Li and G. D. Clifford, “Dynamic time warping and machine learning for signal quality assessment of pulsatile signals,” *Physiol. Meas.*, vol. 33, no. 9, p. 1491, 2012.
- [18] C. Orphanidou, T. Bonnici, P. Charlton, D. Clifton, D. Vallance, and L. Tarassenko, “Signal-Quality Indices for the Electrocardiogram and Photoplethysmogram: Derivation and Applications to Wireless Monitoring,” *IEEE J. Biomed. Heal. Informatics*, vol. 19, no. 3, pp. 832–838, 2015, doi: 10.1109/JBHI.2014.2338351.
- [19] T. Suzuki, K. Kameyama, and T. Tamura, “Development of the irregular pulse detection method in daily life using wearable photoplethysmographic sensor,” in *2009 Annual International Conference of the IEEE Engineering in Medicine and Biology Society*, 2009, pp. 6080–6083.
- [20] G. N. K. Reddy, M. S. Manikandan, and N. V. L. N. Murty, “On-Device Integrated PPG Quality Assessment and Sensor Disconnection/Saturation Detection System for IoT Health Monitoring,” *IEEE Trans. Instrum. Meas.*, 2020.
- [21] T. Pereira *et al.*, “A supervised approach to robust photoplethysmography quality assessment,” *IEEE J. Biomed. Heal. Informatics*, vol. 24, no. 3, pp. 649–657, 2019.
- [22] N. Pradhan, S. Rajan, and A. Adler, “Evaluation of the signal quality of wrist-based photoplethysmography,” *Physiol. Meas.*, vol. 40, no. 6, p. 65008, 2019.
- [23] K. Maharatna, E. B. Mazomenos, J. Morgan, and S. Bonfiglio, “Towards the development of next-generation remote healthcare system: Some practical considerations,” in *2012 IEEE International Symposium on Circuits and Systems*, 2012, pp. 1–4.
- [24] S. V. Vaseghi, *Advanced digital signal processing and noise reduction*. John Wiley & Sons, 2008.
- [25] C. Ding and H. Peng, “Minimum redundancy feature selection from microarray gene expression data,” *J. Bioinform. Comput. Biol.*, vol. 3, no. 02, pp. 185–205, 2005.
- [26] C. Seiffert, T. M. Khoshgoftaar, J. Van Hulse, and A. Napolitano, “RUSBoost: Improving classification performance when training data is skewed,” in *2008 19th International Conference on Pattern Recognition*, 2008, pp. 1–4.
- [27] U. Satija, B. Ramkumar, and M. Sabarimalai Manikandan, “A Review of Signal Processing Techniques for Electrocardiogram Signal Quality Assessment,” *IEEE Rev. Biomed. Eng.*, vol. 11, pp. 36–52, 2018, doi: 10.1109/RBME.2018.2810957.
- [28] J. A. Sukor, S. J. Redmond, and N. H. Lovell, “Signal quality measures for pulse oximetry through waveform morphology analysis,” *Physiol. Meas.*, vol. 32, no. 3, pp. 369–384, 2011, doi: 10.1088/0967-3334/32/3/008.
- [29] W. Karlen, K. Kobayashi, J. M. Ansermino, and G. A. Dumont, “Photoplethysmogram signal quality estimation using repeated Gaussian filters and cross-correlation,” *Physiol. Meas.*, vol. 33, no. 10, pp. 1617–1629, 2012, doi: 10.1088/0967-3334/33/10/1617.
- [30] M. Elgendi, “Optimal Signal Quality Index for Photoplethysmogram Signals,” *Bioeng. (Basel, Switzerland)*, vol. 3, no. 4, p. 21, Sep. 2016, doi: 10.3390/bioengineering3040021.
- [31] S. Vadrevu, S. Member, and M. S. Manikandan, “Real-Time PPG Signal Quality Assessment System for Improving Battery Life and False Alarms,” *IEEE Trans. Circuits Syst. II Express Briefs*, vol. 66, no. 11, pp. 1910–1914, 2019, doi: 10.1109/TCSII.2019.2891636.
- [32] D. Dao *et al.*, “A Robust Motion Artifact Detection Algorithm for Accurate Detection of Heart Rates From Photoplethysmographic Signals Using Time–Frequency Spectral Features,” *IEEE J. Biomed. Heal. Informatics*, vol. 21, no. 5, pp. 1242–1253, 2017, doi: 10.1109/JBHI.2016.2612059.
- [33] A. Galli, C. Narduzzi, and G. Giorgi, “Measuring Heart Rate During Physical Exercise by Subspace Decomposition and Kalman Smoothing,” *IEEE Trans. Instrum. Meas.*, vol. 67, no. 5, pp. 1102–1110, 2018, doi: 10.1109/TIM.2017.2770818.
- [34] M. B. Mashhadi, M. Farhadi, M. Essalat, and F. Marvasti, “Low Complexity Heart Rate Measurement from Wearable Wrist-Type Photoplethysmographic Sensors Robust to Motion Artifacts,” in *2018 IEEE International Conference on Acoustics, Speech and Signal Processing (ICASSP)*, 2018, pp. 921–924, doi: 10.1109/ICASSP.2018.8461520.
- [35] M. A. Motin and S. Member, “PPG Derived Heart Rate Estimation During Intensive Physical Exercise,” *IEEE Access*, vol. 7, pp. 56062–56069, 2019, doi: 10.1109/ACCESS.2019.2913148.
- [36] K. R. Arunkumar and M. Bhaskar, “Robust De-Noiseing Technique for Accurate Heart Rate Estimation Using Wrist-Type PPG Signals,” vol. 20, no. 14, pp. 7980–7987, 2020.